



LAWRENCE  
LIVERMORE  
NATIONAL  
LABORATORY

# Vibrational properties of water under confinement: Electronic effects

D. Donadio, G. Cicero, E. Schwegler, M. Sharma,  
G. Galli

October 22, 2008

Journal of Physical Chemistry

## **Disclaimer**

---

This document was prepared as an account of work sponsored by an agency of the United States government. Neither the United States government nor Lawrence Livermore National Security, LLC, nor any of their employees makes any warranty, expressed or implied, or assumes any legal liability or responsibility for the accuracy, completeness, or usefulness of any information, apparatus, product, or process disclosed, or represents that its use would not infringe privately owned rights. Reference herein to any specific commercial product, process, or service by trade name, trademark, manufacturer, or otherwise does not necessarily constitute or imply its endorsement, recommendation, or favoring by the United States government or Lawrence Livermore National Security, LLC. The views and opinions of authors expressed herein do not necessarily state or reflect those of the United States government or Lawrence Livermore National Security, LLC, and shall not be used for advertising or product endorsement purposes.

# Vibrational properties of water under confinement: electronic effects.

Davide Donadio<sup>1</sup>, Giancarlo Cicero<sup>2</sup>, Eric Schwegler<sup>3</sup>,  
Manu Sharma<sup>1</sup> and Giulia Galli<sup>1</sup>

<sup>1</sup>Department of Chemistry, University of California,  
One Shields Avenue, Davis, CA 95616

<sup>2</sup> Politecnico di Torino, Turin, Italy

<sup>3</sup>Lawrence Livermore National Laboratory, Livermore, CA 94550

August 29, 2008

## Abstract

We compare calculations of infrared (IR) spectra of water confined between non polar surfaces, carried out using *ab initio* and classical simulations. *Ab-initio* results show important differences between IR spectra and vibrational density of state, unlike classical simulations. These differences originate from electronic charge fluctuations at the interface, whose signature is present in IR spectra but not in the density of states. The implications of our findings for the interpretation of experimental data are discussed.

## 1 Introduction

Given the importance of confined water in a variety of scientific fields,<sup>1</sup> ranging from biology<sup>2-5</sup> to materials science,<sup>6-8</sup> many experimental and theoretical studies have been conducted to determine its properties, yet many of them are still the subject of debate.<sup>9-12</sup>

Interpreting experimental results on water in confined media has proven rather difficult in many instances, and firm conclusions based only on experimental observations are sometimes hard to draw. For this reason it is desirable to interpret and complement experimental data by using atomistic simulations. Recently we have undertaken a series of first-principles computational study of the structural properties of water confined between hydrophilic silicon carbide surfaces<sup>13</sup> and non polar surfaces, including graphene

1  
2  
3  
4 sheets, carbon nanotubes<sup>14</sup> and deuterated diamond.<sup>15</sup> For all cases we  
5 found that the perturbation on the water hydrogen bonded network induced  
6 by the confining surfaces is spatially localized within a thin interfacial layer  
7 (( $\sim 0.5$  nm in the case of non polar substrates and slightly smaller, about  
8 0.3 nm in the case of SiC). An important question yet to be fully addressed  
9 is the identification of a set of observables allowing for a clear connection  
10 between simulations and existing and future measurements, thus providing  
11 a robust probe of the fluid under confinement.  
12

13 Here we focus on the vibrational properties of confined water, in par-  
14 ticular its IR spectra. We compare results obtained using *ab initio* and  
15 classical simulations, and we discuss subtle but important electronic effects  
16 contributing to IR signals. Such effects can be accounted for only within  
17 an *ab initio* framework, and are responsible for specific features found in  
18 IR spectra. We chose to compare classical and first principles calculations  
19 in the case of graphene, for which well established empirical, interaction  
20 potentials are available in the literature. Our findings provide guidance in  
21 the interpretation of current and future experimental results, and highlight  
22 the importance of considering all contributions determining an IR signal,  
23 including electronic ones, and not only incomplete information contained in  
24 vibrational density of states. The comparison between IR spectra obtained  
25 with *ab initio* and classical calculations also sheds light on the nature of the  
26 interaction between water molecules and non polar confining surfaces.  
27

28 The rest of the paper is organized as follows: in the next section the  
29 theoretical framework of our classical and *ab initio* simulations is outlined,  
30 and the way we obtained IR spectra from equilibrium molecular dynamics  
31 simulations is described. In section 3 we discuss the *ab initio* results for  
32 water confined between graphene surfaces, and in Sec. 4 we compare them  
33 to the spectra obtained from classical MD simulations. Sec. 5 contains our  
34 conclusions.  
35  
36  
37

## 38 2 Method

39 We carried out molecular dynamics (MD) simulations of water confined  
40 between graphene sheets at distances varying from 1.01 to 2.5 nm, by using  
41 both *ab initio* simulations<sup>15</sup> and classical empirical potentials. In particular,  
42 we used a flexible simple point charge model (SPCF)<sup>16</sup> and a polarizable  
43 model.<sup>17</sup>  
44

45 When performing computer simulations, the preparation of a solid/liquid  
46 interface within a confined medium is not straightforward. The main diffi-  
47  
48  
49  
50  
51  
52  
53  
54  
55  
56  
57  
58  
59  
60

culty lies in estimating the number of water molecules required to fill up the confined space, in the presence of an excluded volume between the surface and the wetting layer. Such volume is not a priori known and eventually has to be subtracted from the volume accessible to water molecules, in order to determine the density of the confined fluid. To compute the number of water molecules, we determined the initial configuration of the system by using classical simulations with a SPC/E<sup>18</sup> potential in all cases. First a trial system (with a tentative number of water molecules) was equilibrated and then MD runs were repeated either by changing the number of water molecules in the confined space or by varying the dimensions of the confining volume until the stress on the simulation cell corresponds to atmospheric pressure conditions. The samples obtained in this way were used as starting points for both *ab initio* and subsequent classical runs. We chose an SPC/E model to prepare our samples because well tested van der Waals parameters to describe the interaction between water and graphite surfaces and nanotubes (NTs) were available in the literature.<sup>19</sup> In particular the carbon atoms were modeled as neutral particles interacting with the oxygen atoms through a Lennard-Jones potential determined by the parameters  $\varepsilon_{CO} = 0.3651$  kJ/mol and  $\sigma_{CO} = 0.319$  Å.<sup>19,20</sup> In the graphene/water system the cell dimensions in the (x,y) plane were fixed and determined by the size of a relaxed graphene sheet containing 60 carbon atoms (12.4×12.1 Å). In the z direction the graphene layer distance was optimized to accommodate 32 water molecules. The thickness of the exclusion volume present at the graphene/water interface, as determined by the atomic density profile  $\rho(z)$ , was estimated to be  $\sim 2$  Å.

In classical simulations<sup>21</sup> of IR spectra we used two different parameterizations of the flexible SPC forcefield,<sup>16,22</sup> and a polarizable force field where the oxygen polarizability is described by a Drude model.<sup>17</sup> In these cases, the IR spectra were computed from the autocorrelation function of the total dipole moment  $\vec{M}$ , which is the sum of the molecular dipoles  $\vec{\mu}_i$ . The dipole of each water molecule for the flexible simple point charge (SPC) models used in the classical simulations is easily defined:  $\vec{\mu}_i = q_O \vec{r}_O + q_H \vec{r}_{H1} + q_H \vec{r}_{H2}$ .

In the first principle MD simulations the interatomic interactions are computed by solving the electronic structure within density functional theory using the generalized gradient approximation by Perdew, Burke and Ernzerhof.<sup>23</sup> We adopted norm-conserving pseudopotentials,<sup>24</sup> and a plane-wave basis set with a cutoff of 85 Ry. In this case, we computed IR spectra using a version of Car-Parrinello (CP)*ab initio* MD<sup>25-27</sup> (AIMD), in which maximally localized Wannier functions (MLWFs),<sup>28</sup> in place of Bloch orbitals, are propagated “on-the-fly”. MLWFs are equivalent to Boys

orbitals<sup>29</sup> used in Quantum Chemistry. Wannier Functions (WF) are obtained from the eigenstates of the Hamiltonian by a unitary transformation and then MLWF are derived from WF by localization in real space. We use a time step of 7 a.u. (0.17 fs) and a fictitious electron mass of 350 a.u. to integrate the electronic and ionic equations of motion.<sup>25</sup> The main advantage of using MLWF is that we can define the dipole moment of a water molecule  $\mu_i$  as:  $\mu_i = e(6\vec{r}_O + \vec{r}_{D_1} + \vec{r}_{D_2} - 2\sum_{l=1,4}\vec{r}_{W_l})$  where  $\vec{r}_{D_1}$ ,  $\vec{r}_{D_2}$  and  $\vec{r}_O$  are the coordinates of the deuterium and oxygen atoms, respectively, and  $\vec{r}_{W_l}$  are the centers of the four (doubly occupied) MLWFs associated to molecule  $i$ . The total polarization is given as the sum of the individual dipole moments of the water molecules and the dipole moment of the surface atoms. The x and y components of the surface dipole have been computed from the atomic and Wannier center coordinates, modulo the "polarization quantum", as in the theory of polarization based on the Berry phase formalism.<sup>30,31</sup>

The IR absorption coefficient per unit length  $\alpha(\omega)$  is related to the refractive index  $n(\omega)$  and the imaginary part of the dielectric constant  $\varepsilon(\omega)$  by  $\alpha(\omega)n(\omega) = (\omega/c)\varepsilon(\omega)$ . Within linear-response theory,  $\alpha(\omega)$  is given by the power spectrum of the time-correlation function of the total dipole operator  $\hat{M}$ . Here we approximate the quantum time-correlation function with the classical one, i.e., with  $\langle M(0)M(t) \rangle$  where  $M$  is the total dipole moment in the simulation cell and the brackets indicate classical ensemble averages. The quantum time-correlation function can be expressed in several equivalent ways, leading to formulae for the IR absorption coefficient characterized by different prefactors; these are known as quantum correction factors. Following Refs.,<sup>32-34</sup> we adopt the so-called harmonic approximation (HA) that is obtained by replacing the Kubo-transformed quantum correlation function with the classical one. The quantum corrected line-shape  $I(\omega)$  is:

$$I(\omega) = \frac{\beta\hbar\omega}{1 - e^{-\beta\hbar\omega}} I_{cl}(\omega) \quad (1)$$

where  $\beta$  is the inverse temperature and  $I_{cl}(\omega)$  is the Fourier transform of the classical  $\langle M(0)M(t) \rangle$ . In the harmonic regime, the HA is exact. Ramirez et al.<sup>33</sup> showed that HA is the only correction factor that satisfies the fluctuation-dissipation theorem in addition to detailed balance. The same authors also found that HA performs better than the other quantum correction factors for one-dimensional anharmonic potentials modeling several, different H-bond scenarios. In Ref.<sup>34</sup> the HA prefactor was shown to provide a good agreement with experiment, for the relative intensities of IR absorption bands of deuterated bulk water computed within the same *ab initio* framework as in the present work.

In the HA the IR absorption coefficient per unit path length of a sample of volume  $V$  is given by:

$$\alpha(\omega)n(\omega) = \frac{2\pi\omega^2\beta}{3cV} \int_{-\infty}^{\infty} dt e^{-i\omega t} \langle \sum_{ij} \boldsymbol{\mu}_i(t) \cdot \boldsymbol{\mu}_j(0) \rangle. \quad (2)$$

All the IR and power spectra presented hereafter have been smoothened by a Fourier filter with a  $50 \text{ cm}^{-1}$  width.

The IR spectra have been computed in microcanonical (constant number of particles, volume and energy, NVE) MD simulations; the *ab initio* and classical runs were 10 and 50 ps long, respectively. Production runs were performed after equilibrating the system at 350 K<sup>35</sup> and at room temperature, in the *ab initio* and classical case, respectively.

The use of a CP scheme to perform *ab initio* MD involves assigning a fictitious mass to the electronic states (MLWF in our specific case) and a fictitious equation of motion for the electrons is solved at each ionic step, without solving self-consistently the Kohn-Sham problem. Values of this fictitious mass must be chosen carefully, for each specific system, in order not to affect significantly the dynamical properties of the simulated sample, and thus obtain results equivalent to those of Born-Oppenheimer (BO) simulations. In BO simulations at each ionic step the electronic ground state is obtained by solving self-consistently the Kohn-Sham problem.<sup>35</sup> To check how the choice of the fictitious electronic mass affects calculations of IR spectra, we performed a CP simulation of a 16 molecule proton disordered model of hexagonal ice, with  $m_e = 350 \text{ a.u.}$  and we compared our results to those obtained by BO molecular dynamics simulations,<sup>14,36</sup> where the MLWF were computed every 1.2 fs (Fig. 1) using the algorithms developed by<sup>37</sup> We observed a red-shift of the high frequency bands computed by CP molecular dynamics, with the shift being larger, the higher the frequency. In the harmonic approximation, if we assign an effective mass  $\mathcal{M}$  to harmonic modes of frequency  $\nu$ , for a fictitious mass  $m_e$ ,  $\nu$  is shifted by  $\Delta\nu$ , such that  $\nu + \Delta\nu = \nu / (1 + m_e/\mathcal{M})^{\infty/\epsilon}$ , with respect to that obtained in BO simulations. Fig. 1 shows that by applying this simple correction term, one achieves good agreement between CP and BO IR spectra, for the value of the fictitious electron mass used in this work. Besides this frequency dependent shift, no significant changes have been observed in the IR line shape of ice computed with CP and BO simulations.

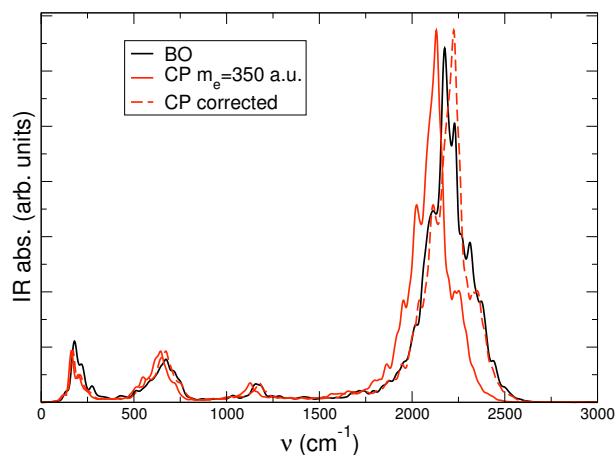


Figure 1: Simulated IR spectrum of ice  $I_h$  by Born-Oppenheimer (black solid line) and Car-Parrinello (red solid line) MD with a fictitious electronic mass  $m_e = 350$  a.u. The Car-Parrinello IR spectrum, corrected by  $\nu + \Delta\nu = \nu / (1 + m_e/M)^{\infty/\epsilon}$  assuming  $M$  equal to the mass of Deuterium is also shown (red dashed line).

### 3 Ab initio IR spectra

In this section we present the IR and power spectra of water confined by graphene sheets (composed of 60 C atoms) at a distance of 1.01 nm and discuss the main features of the IR signal arising from electronic effects. Before doing so, we briefly summarize the structural and electronic properties of the interfacial liquid layer.

The structural properties of confined water found in *ab initio* simulations have been presented in Ref.<sup>14</sup> and <sup>15</sup> where we have shown that in the presence of a surface delimiting liquid water, density oscillations are induced extending few Angstrom from the interface, with an increased density of molecules in close proximity of the surface. In particular, in proximity of a boundary there exists one (or few) layer(s) of water, which is structurally different from the bulk liquid. Interestingly, we found that the properties of this highly perturbed water layer do not depend on surface separation. In addition, even in the case of high, hydrophobic confinement, the perturbation on water structural properties induced by the surface is localized within a layer 0.3-0.5 nm thick. This is consistent with the results of recent investigations<sup>38,39</sup> where experimentally upper bounds to the surface layer were given (varying between 0.25 and 0.6 nm). It has been suggested<sup>10</sup> that



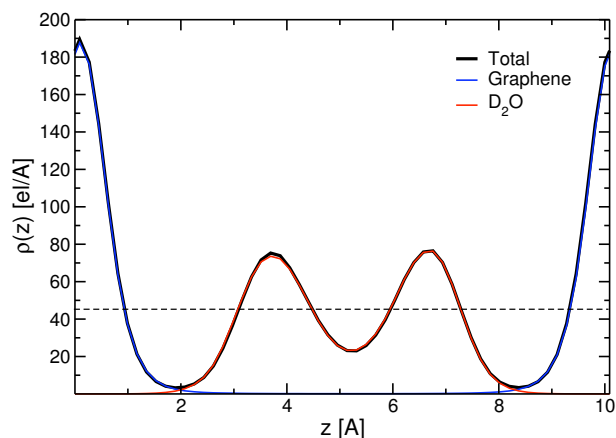


Figure 2: Electron density of the coupled water-graphene system (32 water molecules confined within graphene sheets at a distance of 1.01 nm), as obtained from *ab initio* simulations (see text). The positions of the carbon atoms of the graphene layers are at 0 and 10.1 Å respectively. The red, blue and black curves represent the electronic density of water, graphene and the total density, respectively. The dashed line indicates the average bulk density.

a rarefaction of the density of water is present in proximity of a hydrophobic surface and this topic is still the subject of heated debate. Ref.<sup>10</sup>'s results were recently challenged by Ocko *et al.*<sup>11</sup> and by Kashimoto *et al.*<sup>12</sup> Fig. 2 shows the electronic density as a function of the graphene layer separation as obtained in our calculations. The observed depletion of electronic density in close proximity of the surface (i.e. in a region of linear dimension  $\sim 1$  Å from which water molecules are excluded) does not imply and is not accompanied by a rarefaction of water molecules at the interface. In fact, we find a peak of the mass density of water at the graphene interface, similar to that observed at the deuterated diamond interface,<sup>15</sup> showing the absence of a water molecule depletion layer, consistent with the results of Ref.<sup>12</sup>

In Fig. 3, we report the computed IR spectrum of 32 water molecules in contact with graphene at a confinement of 1.01 nm (red line) and we compare it with computed vibrational density of states (v-DOS) (blue line) and with the IR signal obtained for the coupled water-graphene system (black line). The spectrum shown by the red line has been evaluated by restricting the sum yielding the total dipole moment to the water molecules only, when computing the dipole-dipole correlation function. The position of the

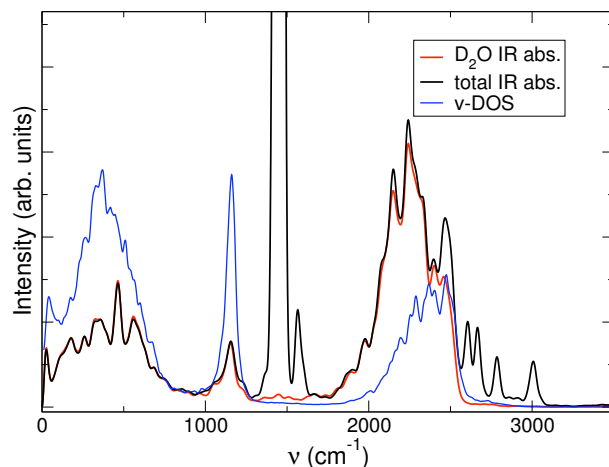


Figure 3: Computed IR spectrum of 32  $D_2O$  molecules confined between graphene sheets at a distance of 1.01 nm. The black and red lines represent the full spectrum ( $D_2O$  plus surface) and that of the water molecules, respectively. The blue line represents the power spectrum of  $D_2O$ , obtained from the Fourier transform of the velocity autocorrelation functions of the D atoms.

lowest frequency peak and of the bending modes is the same in the v-DOS and IR spectra, although the relative peak intensities are different. The main peak of the high frequency modes is instead shifted towards higher frequencies in the v-DOS, compared to IR, indicating a different IR activities of stretching modes, depending on whether OD bonds are engaged in hydrogen bonding and on the character of the hydrogen bonds (donor or acceptor). An analysis of the ionic trajectories shows that the peak of the v-DOS at  $2500\text{ cm}^{-1}$  corresponds to OD bonds not engaged in hydrogen bonding with other molecules, and belonging to molecules in the immediate interfacial region. The feature corresponding to "free" OD bonds in the IR spectrum is much weaker than in the v-DOS, and it appears as a shoulder of the high frequency peak. This indicates that the IR activity of free OD bonds is negligible. This is surprising, as it is well known that stretching modes of a symmetric-top molecules such as water are IR active.

Interestingly the full spectrum (surface plus  $D_2O$ ), represented by the black line in Fig. 3, does show a peak at  $\sim 2500\text{ cm}^{-1}$ . Therefore the difference between the full spectrum and the  $D_2O$  spectrum must come from interactions between water molecules and the surface; indeed we find that in the case of interfacial water molecules, the electronic charge density fluctua-

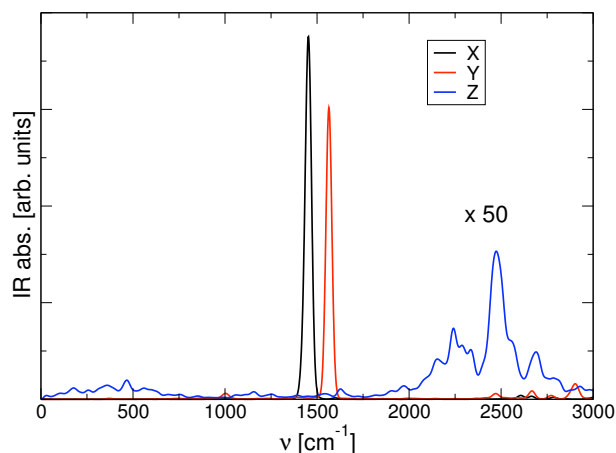


Figure 4: In-plane (X, Y black and red lines) and out-of-plane (Z, blue line) contributions to the graphene sheet IR spectrum, originating from the oscillating dipole of the graphene foils. In the out-of-plane spectrum a correlation with the IR modes of water can be seen by comparing with the results of Fig. 3.

tions at the interface greatly affect the IR activity of O-D bonds not engaged in HB. In particular it is the overlap of the highly polarizable p-electrons of graphene with the electronic charge density of the water molecules that is responsible for the modified IR activity. The intricate interactions of the electrons of graphene with the water molecules are also apparent when decomposing the IR spectrum of the graphene confining surface (Fig. 4). The power spectrum of graphene shows no modes at frequency higher than  $\sim 1600 \text{ cm}^{-1}$ , while the IR spectrum reveals resonances with the IR modes of water.<sup>15</sup> The in-plane spectrum of the surface contains only a single mode (corresponding to the C-C stretch of the graphene layer); the out-of-plane spectrum contains instead a prominent peak at  $\sim 2500 \text{ cm}^{-1}$ , and all of its features correlate well with those observed in the water-graphene spectrum. We emphasize that the high frequency peaks of the graphene spectrum are not related to ionic vibrations but to electronic charge fluctuations induced by the interaction with water.

These results show that an explicit treatment of the electronic structure of the surface and of the liquid is required to understand IR spectra and that interpretation of experimental results based solely on vibrational density of states (or power spectra) does not suffice and may be misleading, as it is shown in the following section, where we discuss results obtained using

classical potentials.

It is interesting to note an analogy between the high frequency features observed in our simulated IR spectra and those reported for hydrogenated water confined in CNTs with very high curvature (diameter of  $\sim 1$  nm).<sup>9</sup> The measurements of Ref.<sup>9</sup> have been interpreted as indicating the presence of a new phase of water under confinement, and in particular of weak inter-ring bonds not present in the bulk. Our calculations show that a peak similar to that reported in Ref.<sup>9</sup> may appear due to charge fluctuations between the OD not involved in hydrogen bonds and the confining surface. Therefore, our results provide a possible, alternative interpretation of the data reported in Ref.<sup>9</sup> In fact water tends to form small rings at hydrophobic (or weakly hydrophilic) surfaces, so as to maximize the number of hydrogen bonds, however without altering the local tetrahedral geometry<sup>40</sup> of the fluid. Although we observed the presence of an increased number of 4- and 5-fold membered rings in confined water, with respect to bulk water, we did not find the occurrence of quasi-planar structures in the interfacial fluid, as suggested in ref.<sup>9</sup>

## 4 Classical MD simulations

In the previous section we have discussed the details of the IR spectra of confined water computed by AIMD simulations. In particular we have shown that accounting explicitly for electronic polarization is essential to achieve a proper description of the interaction between graphene and water, and we have identified the fingerprints of such interaction in IR signals. In classical simulations the surface-water interaction is usually modeled by a Lennard-Jones potential<sup>16,19</sup> that does not include any specific information about the electronic structure of the confining surface, nor about the polarizability of the interfacial water molecules. Here we aim at investigating the impact, on the description of IR spectra, of neglecting the water molecule polarizability, as done in several classical models, or of approximating it *via* a Drude model.

We compared the vibrational density of states obtained from simulations using two different parameterization of the flexible SPC model<sup>16,22</sup> and we conclude that the potential of Ref. <sup>16,41</sup> gives a satisfactory agreement with the power spectrum computed from first principles. In particular, Fig.5 shows that when using this potential there are no qualitative differences between classical MD and AIMD power spectra, except for a small shift of the OD stretching and bending peaks. Based on our results for ice (see Fig.1), we ascribe these differences to inaccuracies of the *ab initio* IR spectra,

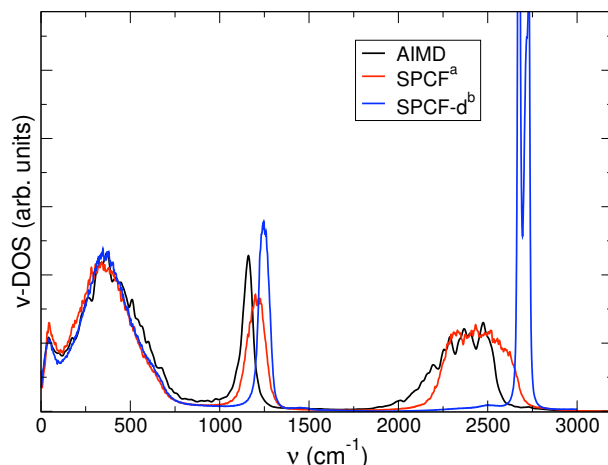


Figure 5: Comparison between the vibrational density of states (v-DOS) of confined water as obtained by using *ab initio* simulations and two different classical force fields: flexible SPC from reference a)<sup>16</sup> and b),<sup>22</sup> respectively.

introduced by the use of a fictitious electron mass in the AIMD simulations. While classical and *ab initio* v-DOS are qualitatively similar, the IR spectra obtained within the two formulations show very important differences both in peak position and relative intensities (see Fig. 6).

As a classical potential does not account for dipole changes occurring in a water molecule upon rigid translation in a charged environment, the low frequency band related to hindered translations ( $\nu$  less than  $250\text{ cm}^{-1}$ ) is absent in the classical IR spectrum. The hindered-libration band is instead much amplified and is by far the most intense peak of the spectrum. This effect is strictly related to the fluid in the confined geometry, and it is much less prominent in the IR of bulk water obtained with the same classical potential (inset of Fig 6). The absence of a hindered translation band and the amplification of the hindered libration most likely stem from the unphysical lack of electrostatic coupling between water and the confining medium. In AIMD calculations the hindered libration band is damped by polarization effects on a given molecules, originating from surrounding water molecules; in a confined geometry the intensity of this band is further damped by the polarization of the confining medium (graphene). Indeed we have shown that the IR activity of graphene layers exhibit modes corresponding to all the IR active modes of water (see Fig. 4). The OD bending peak obtained in classical simulations is also more intense than in the AIMD spectra, again

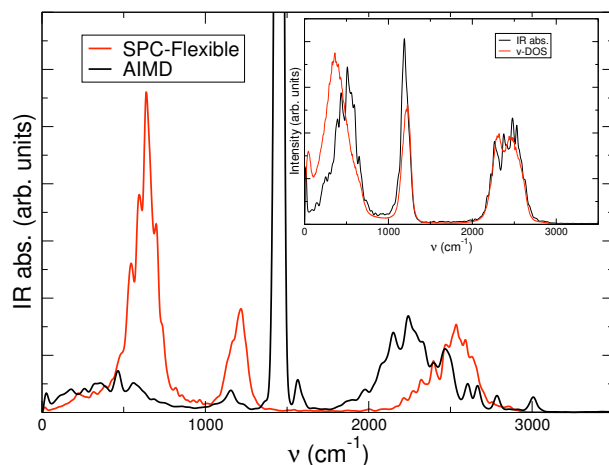


Figure 6: Comparison between classical (red line) and *ab initio* (black line) IR spectra of water confined between two graphene sheets at a distance of 1.01 nm. The inset shows the power spectrum (red) and the IR spectrum (black) of bulk water from classical MD simulations adopting the SPCF force field.<sup>16</sup>

because of lack of polarization effects from the aqueous environment; in this case the confining medium does not appear to play a significant role. The OD bending peak has similar relative intensity in the bulk and in the confined geometry; in addition the corresponding out-of-plane component of the graphene signal, found in the *ab initio* simulation, is rather weak, indicating no substantial coupling between the water molecules and the electrons of graphene. In the high frequency OD stretching band, the mode related to non hydrogen-bonded OD bonds does not appear as a distinct feature in the classical spectrum, however a slight shift of the IR peak towards high frequencies with respect to the bulk is found.

From the comparison shown above we conclude that even when using a flexible point charge potential yielding v-DOS in very good agreement with those obtained *ab initio*, the IR line shapes differ substantially from those found in first principle calculations. This disagreement is due to the fact that classical model potentials do not account for water-surface interactions and polarization effects in a physical sound manner.

A possible route to incorporate polarization effects in a classical simulation is to use a polarizable Drude model. We therefore probed the IR spectrum of bulk and confined water, as described by the polarizable model by Lamoureux *et al.*<sup>17</sup> This model, dubbed SWM4-NDP, is built upon the

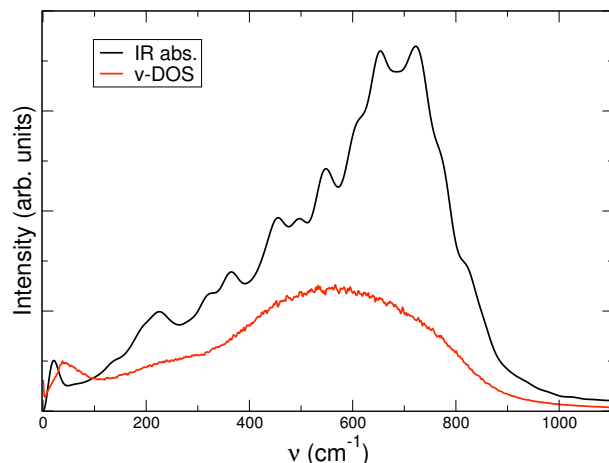


Figure 7: IR spectrum (black line) and vibrational density of states (red) of confined water from classical MD simulations where the polarizable SWM4-NDP potential<sup>17</sup> is adopted.

TIP4P model.<sup>42</sup> The water molecules are treated as rigid bodies with fixed O-H length (0.9572 Å) and HOH angle (104.52°). A massless point charge is placed along the symmetry axis of the molecule in order to account for the permanent dipole moment of water. In addition to this TIP4P like model, the SWM4-NDP force field has a charged shell associated to the oxygen atoms. The oxygen shell and core have opposite charges and therefore account for the effect of a varying dipole. As the water molecules are treated as rigid bodies, by using the SWM4-NDP model we can only probe the far infrared part of the spectrum, which is related to hindered translations and librations. The IR and power spectra of confined water are compared in Fig. 7. At variance with the other classical models considered so far, hindered translational modes are found to be IR active, although the position of the peak in the IR spectrum is shifted with respect to the power spectrum. IR active translational modes have been previously observed for bulk water in Ref.,<sup>43</sup> by using a classical polarizable forcefield, however they differ from those found experimentally and by AIMD,<sup>44</sup> since they obey different selection rules. The ratio of the intensities of translational and librational modes is imbalanced in favor of the latter, this indicates that, as for the SPCF model, a screening term coming from the surface polarization is missing to attenuate the dipole fluctuations along the z axis.

## 5 Conclusions

In summary, we have presented a comparison between IR spectra of water confined within graphene layers, obtained by using *ab initio* and classical simulations. We have shown that in order to describe the interaction of water with non polar surfaces and to account for IR spectra, electronic charge density fluctuations occurring at the interface must be explicitly taken into account. In the near-IR region, *ab initio* vibrational and IR spectra show important differences arising from electronic effects, that is electronic charge fluctuations occurring at the interface. We have also shown that even in the case of classical potentials yielding v-DOS in good, qualitative agreement with *ab initio* results, computed classical and *ab initio* IR spectra differ substantially, due to the lack of a proper account of water-surface interaction and water polarization effects in classical simulations. The use of a polarizable Drude model for water brings classical and *ab initio* simulations into better qualitative agreement, however one should describe also the confining surface as a polarizable system to achieve a satisfactory description of the system.

Finally, our *ab initio* simulations show that all of the notable features found in IR spectra of water confined within graphene layers arise from mere interface effects, i.e. from interactions occurring in close proximity of the interface, and not from new phases of water under confinement.

We gratefully acknowledge support from Scidac grant No. DE-FG02-06ER46262. Part of this work was performed under the auspices of the U.S. Dept. of Energy at the University of California/Lawrence Livermore National Laboratory under contract no. DE-AC52-07NA27344.

This work performed under the auspices of the U.S. Department of Energy by Lawrence Livermore National Laboratory under Contract DE-AC52-07NA27344.



## References

1. Buch, V.; Devlin, J. P. *Water in confining geometries*; Springer Series in cluster physics Springer: Berlin, 2003.
2. Bryant, R. G. *Ann. Rev. Biophys. Biomol. Str.* **1996**, *25*, 29.
3. Israelachvili, J.; Wennerstrom, H. *Nature* **1996**, *379*, 219.
4. Balavoine, F.; Schultz, P.; Richard, C.; Mallouh, V.; Ebbesen, T. W.; Mioskowski, C. *Angew. Chem. Int. Ed.* **1999**, *38*, 1912.
5. Nguyen, C. V.; Delzeit, L.; Cassell, A. M.; Li, J.; Han, J.; Meyyappan, M. *Nano Lett.* **2002**, *2*, 1079.
6. Holt, J. K.; Park, H. G.; Wang, Y.; Stadermann, M.; Artyukhin, A. B.; Grigoropoulos, C. P. *Science* **2006**, *312*, 1034.
7. Majumder, M.; Chopra, N.; Andrews, R.; Hinds, B. J. *Nature* **2005**, *438*, 44.
8. Karaborni, S.; Smit, B.; Heidug, W.; Urai, J.; van Oort, E. *Science* **1996**, *271*, 1102.
9. Byl, O.; Liu, J.-C.; Wang, Y.; Yim, W.-L.; Johnson, J. K.; Yates, J. T. *J. Am. Chem. Soc.* **2006**, *128*, 12090.
10. Poynor, A.; Hong, L.; Robinson, I. K.; Granick, S.; Zhang, Z.; Fenter, P. A. *Phys. Rev. Lett.* **2006**, *97*, 266101.
11. Ocko, B.; Dhinojwala, A.; Daillant, J. *Phys. Rev. Lett.* **2008**, *101*, 039601.
12. Kashimoto, K.; Yoon, J.; Hou, B.; hao Chen, C.; Lin, B.; Aratono, M.; Takiue, T.; Schlossman, M. L. *Phys. Rev. Lett.* **2008**, *101*, 076102.
13. Cicero, G.; Grossman, J. C.; Catellani, A.; G, G. *J. Am. Chem. Soc.* **2005**, *127*, 6830-6835.
14. Cicero, G.; Grossman, J. C.; Schwegler, E.; Gygi, F.; Galli, G. *J. Am. Chem. Soc.* **2008**, *130*, 1871.
15. Sharma, M.; Donadio, D.; Schwegler, E.; Galli, G. *Nano Lett.* **2008**, *in press*.

16. M. C. Gordillo, G. N.; Marti, J. *J. Chem. Phys.* **2005**, *123*, 054707.
17. Lamoureux, G.; MacKerell Jr., A. D.; Roux, B. *J. Chem. Phys.* **2003**, *119*, 5185.
18. Berendsen, H. J. C.; Grigera, J. R.; Straatsma, T. P. *J. Phys. Chem.* **1987**, *91*, 6269-6271.
19. Werder, T.; Walther, J. H.; Jaffe, R.; Halicioglu, T.; Koumoutsakos, P. *J. Phys. Chem. B* **2003**, *107*, 1345-1352.
20. Jaffe, R. L.; Gonnet, P.; Werder, T.; Walther, J. H.; Koumoutsakos, P. *Molecular Simulation* **2004**, *30*, 205-216.
21. Smith, W.; Leslie, M.; Forester, T. R. "DLPOLY version 2.16", CCLRC, Daresbury Laboratory, Daresbury, England.
22. Deng, L. X.; Pettitt, B. M. *J. Chem. Phys.* **1987**, *91*, 3349.
23. Perdew, J. P.; Burke, K.; Ernzerhof, M. *Phys. Rev. Lett.* **1996**, *77*, 3865.
24. Hamann, D. R.; Schluter, M.; Chiang, C. *Phys. Rev. Lett.* **1979**, *43*, 1494.
25. Car, R.; Parrinello, M. *Phys. Rev. Lett.* **1985**, *55*, 2471.
26. Sharma, M.; Wu, Y.; Car, R. *Int. J. Quantum Chem.* **2003**, *95*, 821.
27. <http://www.quantumespresso.org> .
28. Marzari, N.; Vanderbilt, D. *Phys. Rev. B* **1997**, *56*, 12847.
29. Boys, S. F. *Rev. Mod. Phys.* **1960**, *32*, 296.
30. Resta, R. *Rev. Mod. Phys.* **1994**, *66*, 899.
31. King-Smith, R.; Vanderbilt, D. *Phys. Rev. B* **1993**, *47*, 1651.
32. Bader, J. S.; Berne, B. J. *J. Chem. Phys.* **1994**, *100*, 8359.
33. Ramirez, R.; Lopez-Ciudad, T. L.; P, P. K.; Marx, D. *J. Chem. Phys.* **2004**, *121*, 3973.
34. Chen, W.; Sharma, M.; Resta, R.; Galli, G.; Car, R. *Phys. Rev. B* **2008**, *77*, 245114.

35. Grossman, J. C.; Schwegler, E.; Draeger, E. W.; Gygi, F.; Galli, G. *J. Chem. Phys.* **2004**, *120*, 300.
36. Gygi, F. "QBOX version 1.33.3", <http://eslab.ucdavis.edu/software/qbox>.
37. Gygi, F.; Fattebert, J. L.; Schwegler, E. *Comp. Phys. Comm.* **2003**, *155*, 1-6.
38. Mezger, M.; Reichert, H.; Schder, S.; Okasinski, J.; Schroeder, H.; Dosch, H.; Palms, D.; Ralston, J.; Honkimaki, V. *Proc. Natl. Acad. Sci. USA* **2006**, *103*, 18401.
39. Ge, Z.; Cahill, D. G.; ; Braun, P. V. *Phys. Rev. Lett.* **2006**, *96*, 186101.
40. Andreussi, O.; Donadio, D.; Parrinello, M.; Zewail, A. H. *Chem. Phys. Lett.* **2006**, *426*, 115-119.
41. Marti, J.; Padro, J. A.; Guardia, E. *J. Mol. Liq.* **1994**, *62*, 17-31.
42. Jorgensen, W. L.; Chandrasekhar, J.; Madura, J. F.; Impey, R. W.; Klein, M. L. *J. Chem. Phys.* **1983**, *79*, 926.
43. Madden, P. A.; Impey, R. W. *Chem. Phys. Lett.* **1986**, *123*, 502.
44. Sharma, M.; Resta, R.; Car, R. *Phys. Rev. Lett.* **2005**, *95*, 187401.